Determination of refractive index and thickness of a multilayer structure with a single terahertz time domain spectroscopy measurement

Federico Sanjuan,[1,*] Alexander Bockelt,[2] and Borja Vidal[2]

[1]CIOp (Conicet-CIC), cno. Parque Centenario e/505 y 508, Buenos Aires 1897, Argentina

[2]Nanophotonics Technology Center, Universitat Politècnica de València, Camino de Vera, s.n., Valencia 46022, Spain

*Corresponding author: federicosj@ciop.unlp.edu.ar

Received 15 April 2014; revised 19 June 2014; accepted 20 June 2014; posted 23 June 2014 (Doc. ID 210202); published 23 July 2014

A processing technique for the determination of the average refractive index and thickness of a two-layer system is presented. It is based on a single measurement with a standard terahertz time-domain spectrometer and the multilayer system thickness. The technique relies on the interference caused by the main pulse with the echoes produced in each material. This approach allows noninvasive inspection of double-layer compound products. © 2014 Optical Society of America

OCIS codes: (160.4760) Optical properties; (300.6495) Spectroscopy, terahertz; (260.3160) Interference.

http://dx.doi.org/10.1364/AO.53.004910

1. Introduction

The terahertz (THz) region (0.1–10 THz) of the electromagnetic spectrum offers interesting features for nondestructive sensing [1,2]. It holds signatures of a wide range of physical processes, it is nonionizing and there are many materials such as plastics, clothes, papers, etc. that are transparent in this band. Thus, this band can be used for the noninvasive characterization of samples inside packages. In general the capability to analyze multilayered dielectric materials broadens the application field of a sensing technology, especially if the measurement procedure is simple and fast. Multilayer structures are usually analyzed in the optical region [3]. However, many packaging materials are not transparent in this band. Another conventional approach is x-ray inspection [4], which has the risks of using ionizing radiation. THz sensing avoids these limitations.

In the THz band the transfer matrix method can be used to analyze multilayer structures and extract material parameters of a layer within a known multilayer sample [5,6]. To extract the dielectric properties and the thicknesses of a whole multilayer dielectric system, a method based on the relations between a signal transmitted through a reference material at normal incidence and signals transmitted through the material system at different oblique angles of incidence for fitting the theoretical model with the experimental results has been proposed [7]. This approach is similar to variable angle spectroscopic ellipsometry. Although data processing is not too complex, the method requires a number of measurements with different angles, which depend on the number of layers. Another method [8] relies on an algorithm, which, instead of fitting the theoretical model with the experimental transfer function in the frequency domain as shown in [7], uses the temporal domain for fitting the signals. However, it requires simultaneous data extraction in transmission and reflection geometry.

1559-128X/14/224910-04$15.00/0
© 2014 Optical Society of America

In the present work, a data processing technique, which extracts both thicknesses and average refractive indices of a two-layer dielectric material in a single measurement, is developed. This technique is based on the Fourier processing of the Fabry–Perot interference [9,10] and therefore it is suitable for materials that have a constant frequency response of the refractive index (i.e., weakly dispersive materials) in the THz range such as polymers, wood, papers, etc.

2. Theory

The processing technique is based on taking the Fourier transform of the square modulus of the spectrum of the electric field in a conventional transmission THz time-domain spectroscopy setup (THz-TDS).

The theoretical approach is made by assuming normal incidence of the electric field into the sample in transmission geometry, as shown in Fig. 1, although the principle is valid for reflection geometry as well. Figure 1 shows the transmitted and reflected rays for a two-layer material where the thicknesses and refraction indices of both layers are unknown. For this theoretical analysis only one echo is considered in each material. Reflected beams represented by dashed arrows are not considered due to their low amplitude in comparison to other components.

The electric components of the field in the frequency domain after the first material can be written as

$$E_{t1}(\omega) = E_i(\omega)\tau_1(\omega)P_1(\omega)(1 + r_{1\text{-}2}(\omega)r_{1\text{-air}}P_1^2(\omega)), \tag{1}$$

where $E_i(\omega) = |E_i(\omega)|e^{j\vartheta_i(\omega)}$ is the electric component of the field inside the first material,

$$\tau_1(\omega) = \frac{2n_1(\omega)}{n_1(\omega) + n_2(\omega)}, \qquad r_{1\text{-}2}(\omega) = \frac{n_1(\omega) - n_2(\omega)}{n_1(\omega) + n_2(\omega)},$$

$$r_{1\text{-air}}(\omega) = \frac{n_1(\omega) - 1}{n_1(\omega) + 1}, \quad \text{and} \quad P_1(\omega) = e^{-\frac{jn_1\omega d_1}{c}}$$

are the transmission, reflection, and propagation coefficients, respectively, where n_1 and d_1 are the refractive index and sample thickness of the first material.

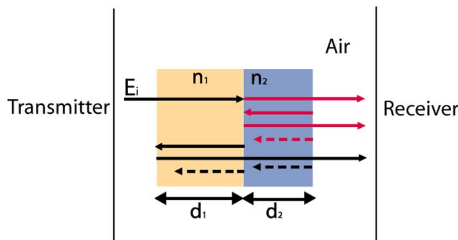

Fig. 1. Electric-field ray tracing in a system made up of two layers with two different thicknesses and refraction indices.

The electric field after the second material is

$$\begin{aligned} E_{t2}(\omega) &= E_{t1}(\omega)\tau_2(\omega)P_2(\omega)(1 + r_{2\text{-}1}(\omega)r_{2\text{-air}}(\omega)P_2^2(\omega)) \\ &= E_i(\omega)\tau_1(\omega)P_1(\omega)\tau_2(\omega)P_2(\omega) \\ &\quad + E_i(\omega)\tau_1(\omega)r_{1\text{-}2}(\omega)r_{1\text{-air}}P_1^3(\omega)\tau_2(\omega)P_2(\omega) \\ &\quad + E_i(\omega)\tau_1(\omega)P_1(\omega)\tau_2(\omega)r_{2\text{-}1}(\omega)r_{2\text{-air}}(\omega)P_2^3(\omega) \\ &\quad + E_i(\omega)\tau_1(\omega)r_{1\text{-}2}(\omega)r_{1\text{-air}} \\ &\quad \times P_1^3(\omega)\tau_2(\omega)r_{2\text{-}1}(\omega)r_{2\text{-air}}(\omega)P_2^3(\omega), \end{aligned} \tag{2}$$

where $\tau_2(\omega)$, $\tau_{2\text{-}1}(\omega)$, $\tau_{2\text{-air}}(\omega)$, and $P_2(\omega)$ are the transmission, reflection, and propagation coefficients of the second material, respectively, with n_2 and d_2 being its refractive index and thickness, respectively. The amplitude of the last term of Eq. (2) is negligible, since it corresponds to the echo created in the second material by the echo generated in the first one and thus is of very small amplitude.

Equation (3) is obtained by taking the squared modulus of Eq. (2) and assuming that the refractive index and the electric field are constant in frequency:

$$\begin{aligned} |E_{t2}(\omega)|^2 &= H_1(n_1,n_2) + H_2(n_1,n_2)\cos\left(\frac{2n_1\omega d_0}{c}\right) \\ &\quad + H_3(n_1,n_2)\cos\left(\frac{2n_2\omega d_2}{c}\right) \\ &\quad + H_4(n_1,n_2)\cos\left(\frac{2w}{c}(n_1d_1 - n_2d_2)\right). \end{aligned} \tag{3}$$

By defining $C_1 = \tau_1\tau_2r_{1\text{-}2}r_{1\text{-air}}$, $C_2 = \tau_1\tau_2$, and $C_3 = \tau_1\tau_2r_{2\text{-}1}r_{2\text{-air}}$ the coefficients $H_i(n_1,n_2)$ can be written as

$$H_1 = C_1^2 + C_2^2 + C_3^2, \qquad H_2 = 2C_1C_2, \qquad H_3 = 2C_2C_3, \qquad H_4 = 2C1C_3.$$

Applying the Fourier transform to Eq. (3) yields

$$\begin{aligned} I(t) &= \mathrm{FT}(|E_{t2}(\omega)|^2) \\ &= H_1(n_1,n_2)\delta(t) + \frac{H_2(n_1,n_2)}{2}\delta\left(t - \frac{2n_1d_1}{c}\right) \\ &\quad + \frac{H_3(n_1,n_2)}{2}\delta\left(t - \frac{2n_2d_2}{c}\right) \\ &\quad + \frac{H_4(n_1,n_2)}{2}\delta\left(\frac{2w}{c}|n_1d_1 - n_2d_2|\right). \end{aligned} \tag{4}$$

The analysis of the signal obtained in Eq. (4) shows that the Dirac deltas' positions provide relations between the material's refractive indices and thicknesses. However, only two of these relations are independent equations, since the fourth term is a linear combination of two of the remaining. By taking the ratio of the second and third term's amplitudes, a third independent equation is obtained that links the variables. The equation system formed by

Eqs. (5)–(8) is used to obtain the unknown variables that characterize the two-layer material (n_1, n_2, d_1, d_2), where d in Eq. (8) is given by the measurement of the thickness of the whole multilayer structure.

$$T_1 = \frac{2n_1 d_1}{c}, \tag{5}$$

$$T_2 = \frac{2n_2 d_2}{c}, \tag{6}$$

$$\frac{H_2(n_1, n_2)}{H_3(n_1, n_2)} = \frac{r_{1\text{-air}}(\omega)}{r_{2\text{-air}}(\omega)} = \frac{(n_1 - 1)(n_2 + 1)}{(n_1 + 1)(n_2 - 1)}, \tag{7}$$

$$d = d_1 + d_2. \tag{8}$$

Since the experimental traces are finite in time, peaks with a certain width will be obtained instead of Dirac delta functions. This broadening limits the resolution of the approach. Figure 2 shows a numerical simulation with $n_1 = 3.5, n_2 = 1.82, d_1 = 670$ μm, $d_2 = 1570$ μm and assuming measurements with a bandwidth up to 1 THz.

In Fig. 2 the four pulses represented by Eq. (4) can be seen, where the upper pulses give T_1, T_2, H_2, and H_1, which are the values used for solving the equation system. Errors in the parameter extraction are induced by errors in the thickness measurement, the spectrometer bandwidth and by the noise that affect the peaks amplitudes. To assess the effect of amplitude noise on the extracted parameters, simulations adding Gaussian noise to the signal considering a system with a signal to noise ratio of 30 dB have been carried out. The variation obtained in the final results was smaller than 0.2%.

3. Experiment

A THz spectrometer in transmission geometry formed by a mode-locked femtosecond laser, a pair of photoconductive antennas and a lock-in amplifier was used for testing the proposed method. The measurements were carried out over a temporal window of 40 ps with a time step of 100 fs. The two-layer structure was made up by a sample of polymer [polybutylene terephthalate (PBT)] and a silicon wafer.

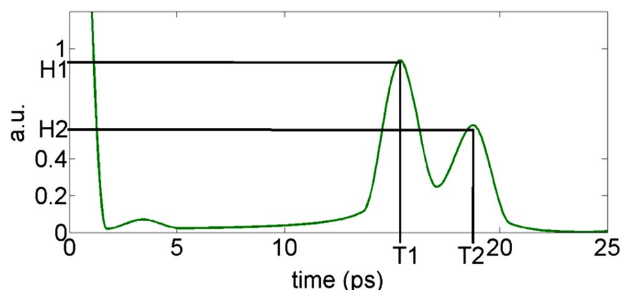

Fig. 2. Numerical simulation of the discrete Fourier transform (DFT) applied to Eq. (3).

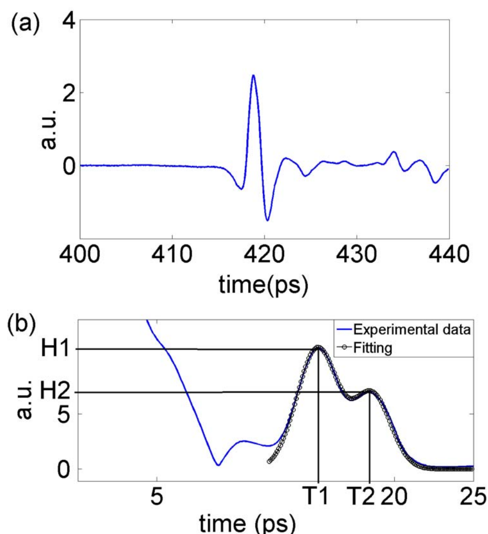

Fig. 3. (a) Time-domain measurement from the THz spectrometer. (b) Outcome of double Fourier processing of the temporal trace shown in (a).

Figure 3(a) shows the time domain trace from the spectrometer. It shows the main temporal pulse and two peaks showing reflections around 434 and 437 ps.

Figure 3(b) shows the result of applying double Fourier processing on the temporal trace shown in Fig. 3(a). The figure shows two peaks in addition to the pulse at 0 ps instead of the three represented by Eq. (4) and shown in Fig. 2. That is because the peak corresponding to the last term of Eq. (4) is given by the difference between the temporal delays introduced by each material and when T_1 and T_2 are similar, $T_2 - T_1$ is close to zero. Depending on the available bandwidth of the experiment it may overlap with the peak at zero, which corresponds to the first term of Eq. (4). It can also be seen in Fig. 3(b) that both peak amplitudes (H_1, H_2) used for obtaining the unknown parameters are affected by the tails of the overlapped pulses due to the lack of resolution. To improve accuracy, the signal is fit with the sum of two Gaussian functions [Fig. 3(b)]. From this the amplitudes are derived.

Thus, in order to obtain the unknown parameters we apply Eqs. (5)–(8) with the values extracted from Fig. 3(b) (T_1, T_2), with the peak amplitudes values of the Gaussian functions and the width of the multilayer structure measured with a digital caliper:

$$T_1 = 15.4 \text{ ps}, \qquad T_2 = 18.9 \text{ ps}, \quad H_1/H_2 = 1.9, \quad d = 2220 \text{ μm}.$$

By numerically solving the system of equations two results are obtained. Only one of these is a viable solution since the other provides complex refractive indexes or indices smaller than one. The resulting values are: $n_1 = 3.48$, $n_2 = 1.82$, $d_1 = 664$ μm, $d_2 = 1556$ μm.

The experimental error can be calculated numerically by adding the dispersion due to the temporal resolution and the sample width error to the extracted parameters. Replacing T_1 by $T_1 \pm 50$ fs, T_2 by $T_2 \pm 50$ fs and d by $d \pm 10$ μm in the equation system, the dispersion found in the solution was $\Delta n_1 = \pm 0.11$, $\Delta n_2 = \pm 0.06$, $\Delta d_1 = \pm 11$ μm and $\Delta d_2 = \pm 16$ μm.

These parameters were verified by measuring each sample's refractive index with conventional processing [2] and the thickness with a digital caliper. The average refractive indices were 3.5 and 1.8 for the silicon wafer and PBT polymer respectively, while their thicknesses were 670 and 1570 μm. Thus, the values obtained with the proposed method are in correspondence with the values provided by a conventional data extraction algorithm applied to each material independently.

4. Conclusion

A simple method to simultaneously determine the optical material parameters and thicknesses of a two-layer structure with constant refractive indices in a single measurement without the need of a reference measurement has been derived and demonstrated. The method is based on a conventional THz-TDS transmission setup and the measurement of the thickness of the whole multilayer structure. When the samples do not have a constant refractive index in the THz band, the result will be an average index, which can be used as initial value for other algorithms. The proposed technique may be useful for nondestructive characterization of composite materials, semiconductor wafers, etc.

The authors thank the Spanish Ministerio de Economia y Competitividad for partially supporting this work through project TEC2012-35797. Federico Sanjuan also thanks Dr. Jorge Tocho and Dr. Alberto Lencina for their encouragement and support.

References

1. B. M. Fischer, H. Helm, and P. U. Jepsen, "Chemical recognition with broadband THz spectroscopy," Proc. IEEE **95**, 1592–1604 (2007) .
2. P. U. Jepsen, D. G. Cooke, and M. Koch, "Terahertz spectroscopy and imaging—modern techniques and applications," Laser Photon. Rev. **5**, 124–166 (2011).
3. H. G. Tompkins and E. A. Irene, eds., *Handbook of Ellipsometry*, (Springer, 2005).
4. A. Yu. Nikulin and P. V. Petrashen, "Practical applications of optical inverse problem technique to characterization of multilayers," in *Proceedings of Advances in X-ray Analysis (AXA), Denver X-ray Conference* (1997), Vol. **41**, pp. 155–164.
5. S. E. Ralph, S. Perkowitz, N. Katzenellenbogen, and D. Grischkowsky, "Terahertz spectroscopy of optically thick multilayered semiconductor structures," J. Opt. Soc. Am. B **11**, 2528–2532 (1994).
6. R. Wilk, I. Pupeza, R. Cernat, and M. Koch, "Highly accurate THz time-domain spectroscopy of multilayer structures," IEEE J. Sel. Top. Quantum Electron. **14**, 392–398 (2008).
7. J. A. Hejase, E. J. Rothwell, and P. Chahal, "A multiple angle method for THz time-domain material characterization," IEEE Trans. THz Sci. Technol. **3**, 656–665 (2013).
8. A. Brahm, A. Weigel, S. Riehemann, G. Notni, and A. Tünnermann, "Highly precise parameter extraction of thin multilayers in THz transmission and reflection geometry," in *Proceedings of IEEE Conference on Infrared, Millimeter and Terahertz Waves*, Houston, 2011, pp. 1–2.
9. F. Sanjuan and B. Vidal, "Refractive index calculation from echo interference in pulsed terahertz spectroscopy," Electron. Lett. **50**, 308–309 (2014).
10. F. Sanjuan, A. Bockelt, and B. Vidal, "Birefringence measurement in the THz range based on double Fourier analysis," Opt. Lett. **39**, 809–812 (2014).